OSMOSE

OPTIMAL SYSTEM-MIX OF FLEXIBILITY SOLUTIONS FOR EUROPEAN ELECTRICITY

Multi-service control algorithm for converters

Deliverable number: D3.1

Contact: www.osmose-h2020.eu

The project has received funding from the European Union's Horizon 2020 research and innovation programme under grant agreement No 773406

Document properties

Project information

Programme	Optimal System-Mix Of Flexibility Solutions For European Electricity
Project Acronym	OSMOSE
Grant agreement	773406
Number of the Deliverable	D3.1
WP/Task related	3

Document information

Document Name	**Multi-service control algorithm for converters**
Date of Delivery	December 17, 2018
Status and version	
Number of Pages	25

Responsible

Responsible	Fabrizio Sossan (fabrizio.sossan@epfl.ch)
Authors	Emil Namor, Fabrizio Sossan, Rachid Cherkaoui, Mario Paolone (Distributed Electrical Systems Laboratory, EPFL, Lausanne, Switzerland)
Reviewers	
Approver	

Dissemination level

Type (distribution level)	**PU Public**
	~~CO – full consortium, Confidential, only for members of the consortium (including the Commission Services)~~
	~~CO – some partners, Confidential, only for some partners (list of partners to be defined)~~

Review history

Version	Date	Reviewer	Comment
V0	November 30, 2018	Marie-Sophie Debry (RTE)	
V1	December 5, 2018		

Contents

List of Figures

List of Tables

Executive Summary

Thanks to their high power ramping and bidirectional power flows, grid-connected battery energy storage systems (BESSs) are a promising technology for supporting the integration of renewable energy in the grid. A key aspect of operating grid-connected BESSs is the ability of providing multiple ancillary services at the same time. This is with the objective of, first, maximizing the exploitation of the power rating of the converter and the full energy capacity of the battery, and, second to increase their profitability by bidding on multiple ancillary services markets. In this report, **we describe a scheduling and control framework for a grid-connected BESS to provide simultaneously multiple services to the electrical grid**. **Its objective is to maximize the battery exploitation from these services in the presence of uncertainty** (i.e., load, stochastic distributed generation, grid frequency). The framework is structured in two phases. In a period-ahead phase, we solve an optimization problem that schedule the allocation of multiple services based on the notion of power and energy budget of each of them. In the subsequent real-time phase the control set-points for the deployment of such services are calculated separately and superimposed. The control framework is first formulated in a general way that can accommodate any kind of services by preliminary computing the power and energy budgets. To show the applicability of the proposed algorithm in a real-life reduced-scale application and although not in the scope of the OSMOSE project, the proposed framework is applied to the problem of dispatching a medium voltage feeder in conjunction to primary frequency control. It is validated by simulations and experiments, performed with a grid-connected 560 kWh/720 kVA Li-ion battery energy storage system connected to the 20 kV grid of the EPFL campus in Lausanne, Switzerland.

List of Acronyms

BESS ..... Battery energy storage system
PV ..... Photovoltaic
AS ..... Ancillary service
LO ..... Local objective
PFR ..... Primary frequency regulation
MV ..... Medium voltage
LV ..... Low voltage
PMU ..... Phasor measurement unit
SOE ..... State of energy

1.Introduction

1.1. Motivations

Battery energy storage systems (BESSs) are a promising technology due to their inherent distributed nature, their ability to inject bidirectional power flows, their high power ramping and ability to provide a set of different grid services. As of today, BESSs are being deployed to provide several different services, such as peak shaving [1], energy management of microgrids [2] and stochastic resources [3,4] and frequency and voltage regulation [5, 6]. Such deployment is still slowed down by the high cost of these devices. While this cost is decreasing due to technological developments and economies of scale, a viable approach to optimize the exploitation of such devices is the development of control strategies able to provide simultaneously more than one of the services listed above. This allows for a better exploitation of the BESS from a technical and economical point of view. More specifically, the simultaneous provision of multiple services via BESSs is of interest with respect to two aspects. First, different applications have different energy and power requirements. Some are "energy intensive", i.e. they need a large amount of energy but low instanteous power (e.g. peak shaving). Other are "power intensive", i.e. require higher levels of power but not high amount of energy (e.g. primary frequency regulation, grid forming and synchronisation strategies) [7, 8]. Such different services could be coupled to match at best the energy and power ratings of the batteries. Second, batteries are normally sized to provide a single service continuously. However, the actual daily deployment of power and exploitation of energy capacity vary due to the uncertainty of the stochastic resources to which they are coupled e.g. uncontrollable loads and PV generation in [3]), or of the pricing signals that they track (e.g. energy and balancing power prices in [9]). Therefore, the deployment of such services rarely requires the exploitation of the whole BESS capacity. When a portion of the BESS's energy capacity remains unexploited by the deployment of its main service, it could be allocated to a secondary service, to be deployed in parallel. In other words, coupling multiple services together may allow to exploit at best the batteries coupled with stochastic resources.

1.2. Literature Survey

The relevance of application sinergies for energy storage devices has been pointed out in general terms in [10]. Several works, in the existing technical literature, propose approaches to provide simultaneously multiple grid services and demonstrate their effectiveness by simulations [9, 11–21]. These references differ from each other for the kind of services they provide and how they account for BESS operational constraints. BESS services can be classified in 3 mainstream categories:

1. energy arbitrage (EA), i.e. buying and selling electricity to generate a revenue;
2. provision of ancillary services (AS). These are a set of services that batteries can provide to grid operators to enhance the system reliability (e.g. frequency response and regulation). The provision of these services is normally regulated by auction based systems and markets;
3. achievement of control objectives for the local grid (i.e. local objectives (LO)), like congestion management, voltage regulation at LV and MV level or self-consumption.

The applications described in [9, 11–21] are designed to provide combinations of the aforementioned services, as summarized in Table 1.1.

In such references, operation scheduling problems for energy storage systems considering multiple services are formulated. These aim at maximising the economic revenue generated for a standalone storage systems exploiting multiple revenue streams. This objective is sought in different pricing contexts and the common result is that by jointly providing multiple services, the BESS economic income

Table 1.1: Recent literature on clustering of BESS applications in power systems

Services provided	References
EA + AS	[9, 11–15]
LO + AS	[16–18]
LO + EA + AS	[19–21]

is increased. Nonetheless, energy storage systems are often used in two further configurations [13]: *i)* used by system operators to improve system reliability (e.g. [22, 23]) or *ii)* in conjunction with other resources such as distributed generation [24], flexible demand [25] or electric vehicles [26].

Besides the objective of the proposed scheduling problems, the references listed in Table 1.1 focus on different aspects of the control framework needed to provide multiple services simultaneously. Several references propose specific methods for storage technologies other than BESSs: compressed air energy storage [14], fleets of thermostatically controlled loads [17], or fleets of distributed BESSs [16]. References [17] and [18], besides the formulation of the scheduling problem, describe the real-time control to implement the proposed strategies. References [12, 13, 18] propose a robust optimization approach to deal with uncertainties related to price signals and reserve deployment. Finally [12] analyses how providing multiple services simultaneously affects the BESS life time.

1.3. Innovations described in this report

We consider the case of a BESS installed in a distribution feeder supplying uncontrollable loads and integrating a considerable amount of distributed generation. The scheduling problem of such BESS consists in allocating portions of its power and energy capacity to achieve different technical objectives, such as the dispatch of the active power demand of the feeder and the provision of primary frequency regulation power to the upper grid layer. Although the proposed framework can be adapted to maximise the revenue coming from providing difference ancillary services in a price-taking setting (as shown in Appendix A), it is formulated with the objective of maximising the capacity of providing ancillary services. The reason for this is that the price taking assumption is not scalable with the number of units participating in the markets. In other words, if many units were to participate in the ancillary services market, an open-loop price signal would not be representative of their aggregated reaction. Recent works in [27] and [28] addresses the problem of decision making for battery systems in a price-setting context, but they solely focus on energy arbitrage, whereas we consider multiple simultaneous services.

Specifically, we focus on the problem of jointly dispatching the operation of an active distribution feeder and provide primary frequency regulation. We provide first a formulation of a general control framework for the provision of multiple simultaneous grid services via BESSs, i.e. a formulation that is agnostic to the services that are provided. This solution does not require coordination mechanisms with other resources or with the upper grid layer nor an extensive communication infrastructure and can be considered as a bottom-up approach to augment the ability of BESSs to provide useful services to the grid. The proposed control has two time layers: (i) a period-ahead and (ii) a real-time one. In the first, we solve an optimization problem that allocates a power and an energy budgets to each considered service. This is done to maximize the exploitation of the BESS energy capacity and ensure continuous operation by managing the BESS stored energy. In the real-time stage, the power setpoints needed for each service are computed independently and superimposed. Based on such general framework, we describe then a BESS control scheme for dispatching the operation of a distribution feeder, such as in [3] and for primary frequency regulation. We show the performance of

this control both in simulations and via experimental results obtained by implementing the proposed framework to control a grid-connected 560 kWh/720 kVA BESS.

With respect to the existing literature, the innovations described in this report are:

- the formulation of a complete algorithmic toolchain to control a BESS in order to provide multiple services simultaneously. This framework differs from the existing literature in: *i)* the generic formulation of the scheduling problem, *ii)* the technical rather than revenue-driven control objective, *iii)* the consideration of the stochastic behaviour of the services deployment (due to the uncertainties in the forecast of the feeder prosumption as well as in the energy needed to perform PFR) and exploitation of robust optimization techniques to hedge against uncertainty and achieve reliable real-time operation (similarly to [13]).
- the formulation of a control strategy to manage a BESS connected within a MV feeder, together with a set of heterogeneous resources (loads and PV generations), in order to dispatch the operation of the same feeder and exploit the remaining capacity to provide PFR.
- the experimental validation of the proposed control tool-chain, providing solid empirical evidences on the applicability, actionability, and performance of the proposed scheduling and control algorithms. In the best of the Authors' knowledge, this is the first work providing such experimental validation for a BESS control scheme considering multiple simultaneous services.

The report is organised as follows. Section 2 presents the general formulation of the control problem of providing multiple services simultaneously via a BESS. Section 3 casts the proposed framework in the specific context of the provision of power for dispatching the operation of an active distribution feeder and for primary frequency regulation (PFR). Section 4 presents results, obtained both via simulations and experiments, that validates the proposed framework. Section 5 discusses how other services, among which synchronization, can be added in the proposed scheduling framework. Finally, Section 6 summarizes the original contributions and main outcomes of the paper and proposes directions for further research.

2.Problem formulation

2.1. Power and energy budgets

We consider the problem of scheduling the operation of a BESS with energy capacity E_{nom} and maximum power P_{max}, for a time window T. During each time window, the BESS provides J services, each denoted by the subscript $j = 1, \dots, J$.

Each service j is characterized by an energy budget $\mathcal{E}_j$ and a power budget $\mathcal{P}_j$. These are the shares of the BESS energy capacity and power necessary along the time window T to deploy the service j. The power and energy budgets $\mathcal{P}_j$ and $\mathcal{E}_j$ necessary for each service are functions of a set of tunable control parameters (composing the decision vector of the scheduling problem and hereafter denoted by x) as well as of variables modelling the uncertainty of the operating conditions related to each service (hereafter θ). The dependency of $\mathcal{P}_j$ and $\mathcal{E}_j$ on θ is introduced to account for the fact that the deployment of the considered services need to be ensured in the occurrence of any scenario of their power demand (practical examples are provided in Section 3). We formulate an optimization problem to determine the value of decision vector x (and hence the power and energy budgets $\mathcal{P}_j$ and $\mathcal{E}_j$ for $j = 1, \dots, J$) that maximizes the portion of BESS energy capacity made available for the provision of the services in J. We discretize the window of duration T in N time steps of duration T/N, each denoted by the subscript k, with $k = 1, \dots, N$. Formally, the power budget of the service j at time step k is denoted $\mathcal{P}_{j,k}$ and is defined as the interval of the expected power values that the service could require at k. These are between the minimum and maximum expected power realizations for

that service, namely in the interval $\mathcal{P}_{j,k} = \left[P^{\downarrow}_{j,k}, P^{\uparrow}_{j,k}\right]$. The power budget along a time period T is defined as the sequence of such intervals:

$$\mathcal{P}_j = \left\{ \left[P^{\downarrow}_{j,k}(x,\theta), P^{\uparrow}_{j,k}(x,\theta)\right], k = 1, \ldots, N \right\}. \tag{2.1}$$

Similarly, the application will require an energy budget

$$\mathcal{E}_j = \{ \left[E^{\downarrow}_{j,k}(x,\theta), E^{\uparrow}_{j,k}(x,\theta)\right], k = 1, \ldots, N \}. \tag{2.2}$$

The power and energy budgets are characterized in terms of their respective envelope, represented in turn by its upper and lower time series:

$$w(\mathcal{E}_j(x,\theta)) = \{E^{\uparrow}_{j,k}(x,\theta) - E^{\downarrow}_{j,k}(x,\theta), k = 1, \ldots, N\}. \tag{2.3}$$

2.2. Composability of power and energy budgets

We introduce the notion of composability of power and energy budgets by defining their sum over the different services to provide. Using the energy budget as example, it is:

$$\sum_j \mathcal{E}_j(x,\theta) = \left\{ \left[\sum_{j=1}^{J} E^{\downarrow}_{j,k}(x,\theta), \sum_j E^{\uparrow}_{j,k}(x,\theta) \right], k = 1, \ldots, N \right\}. \tag{2.4}$$

2.3. Scheduling problem

The problem of providing multiple concurrent services with a BESS, while ensuring feasible operation can now be formulated in generic terms. We seek to maximise the set of widths of the energy budget resulting from the sum of the energy budgets $\mathcal{E}_j$ with $j = 1, \ldots, J$, within a given time window T, while respecting the BESS's capacity and converter power rating. The resulting decision problem is:

$$x^o = \arg\max_x \left|\left| w\left(\sum_{j=1}^{J} \mathcal{E}_j(x,\theta) \right) \right|\right|_1 \tag{2.5}$$

subject to the total energy demand of all the services (i.e., sum over j) should not exceed the battery energy capacity

$$E_{init} + \sum_{j=1}^{J} \mathcal{E}_j(x,\theta) \in [E_{min}, E_{max}], \tag{2.6}$$

and total power demand should be within the power converter's limits (assuming to provide active power only)

$$\sum_{j=1}^{J} \mathcal{P}_j(x,\theta) \in [-P_{max}, P_{max}]. \tag{2.7}$$

It is worth noting that it is possible to have a different objective function while exploiting the same framework presented here. In Appendix A, two variations seeking respectively the maximisation of

the economical revenue and simple feasibility of operation are shown.

2.4. Example of energy and power budgets

Fig. 2.1 shows an illustrative example of the power and energy budgets for a certain service j. Let P_{jks} be the predicted power demand for service j in scenario s. The envelope of the power budget in the upper panel plot of Fig. 2.1 is calculated, for each time interval, as the highest and lowest possible values among all the scenarios:

$$P_{jk}^{\uparrow} = \max_{s}\{P_{jks}\} \tag{2.8}$$

$$P_{jk}^{\downarrow} = \min_{s}\{P_{jks}\}. \tag{2.9}$$

As far as the energy budget is concerned, let us first define E_{jks} as the accumulated energy demand for service j at time t and scenario s. It is calculated by integrating the power demand $P_{j0s}, \ldots, P_{j(k-1)s}$ over time ([1]):

$$E_{jks} = T_s \cdot \sum_{t}^{k-1} P_{jts} \tag{2.10}$$

where T_s is the sampling time. The envelope of the energy budget in the upper panel plot of Fig. 2.1 is given by the worst-case highest and lowest realization of the energy demand over all the scenarios:

$$E_{jk}^{\uparrow} = \max_{s}\{E_{jks}\} \tag{2.11}$$

$$E_{jk}^{\downarrow} = \min_{s}\{E_{jks}\}. \tag{2.12}$$

We note that the formulation in (2.10)-(2.12) differs than calculating the energy budget's envelope as the integral over time of the power budget's envelopes (2.8) and (2.9), i.e.:

$$E_{jk}^{\uparrow} = T_s \cdot \sum_{t}^{k-1} P_{jt}^{\uparrow} \tag{2.13}$$

$$E_{jk}^{\downarrow} = T_s \cdot \sum_{t}^{k-1} P_{jt}^{\downarrow}. \tag{2.14}$$

This explains why the boundaries of the energy budget envelope in Fig. 2.1 are not monotonic. The approach in (2.10)-(2.12) is to prefer over this last as it leads to less conservative estimates of the energy demand.

3.Concurrent dispatch of a MV distribution feeder and primary frequency control

The scheme proposed in Section 2 is now applied to control a BESS to dispatch of a MV distribution feeder and to provide PFR to the grid. We have observed that the battery capacity needed to dis-

[1]We assume unitary efficiency of the charging/discharging process. For battery energy storage systems, this is a good approximation due to their high round-trip efficiency, however it should be re-considered for less efficient energy storage technologies, like fuel cell/electrolyzer systems.

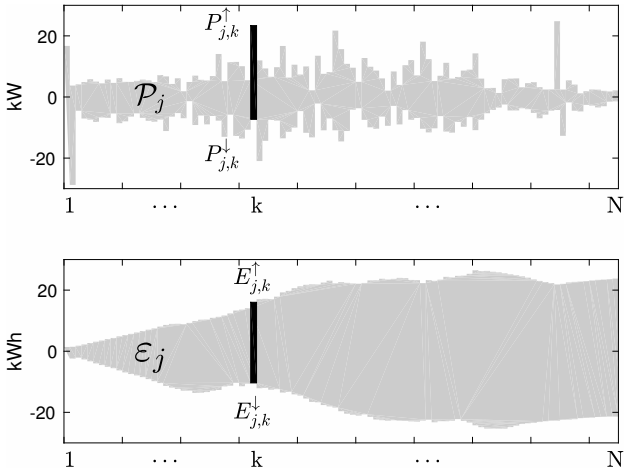

Figure 2.1: Example of power (upper panel) and energy budgets (lower panel) for a service j.

patch a MV feeder as in [3] depends on the uncertainty of the forecast of the connected stochastic resources (loads and stochastic distributed generation). Whereas in some cases the battery capacity is barely sufficient to achieve this goal, in others a considerable portion of the battery capacity remains unutilized when the uncertainty of the prosumption forecast is small.

The choice of PFR as a second stacked service is because *i)* large ramping duties of BESSs accomodate the increased demand for fast regulating power in power systems with a high penetration of production from renewables and *ii)* PFR is a “power intensive” application and is well-suited to be coupled with the dispatch service, which is instead “energy intensive”.

3.1. Day-ahead problem formulation

We want to operate a grid-connected BESS to dispatch the active power flow of a MV distribution system with heterogeneous resources, as in [3], while providing also primary frequency regulation to the grid. Figure 3.1 shows the main features of this setup. The operation is performed over a T=24

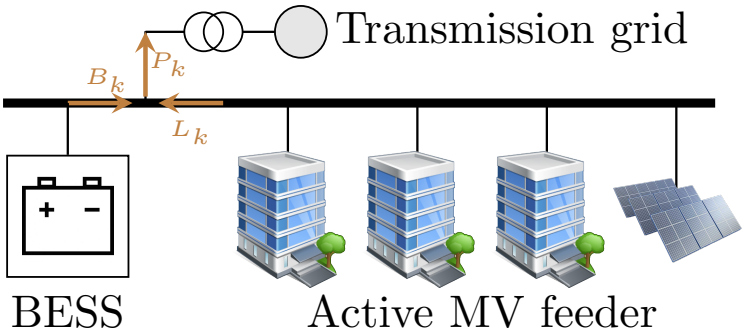

Figure 3.1: Schematic of the experimental setup. The notation of the power flows refers to the real-time control described in section 3.2.

hour period and planned every day for the next calendar day. Following the formulation presented in Section 2, we first define the power and energy budgets for the dispatch and PFR, namely $\mathcal{P}_D$, $\mathcal{P}_{FR}$, $\mathcal{E}_D$ and $\mathcal{E}_{FR}$. Based on these budgets, we formulate an optimization problem as in (2.5)-(2.7).

3.1.1. Power and energy budgets

The dispatch service requires the battery to compensate for the mismatch between the aggregated prosumers power flow, denoted by $\mathbf{L}_k = L_1, \ldots, L_N$, and a pre-established dispatch plan, denoted by $\hat{\mathbf{P}}_k = \hat{P}_1, \ldots, \hat{P}_N$, defined at 5-minutes resolution and computed, for instance, day-ahead. The best guess one could do to dispatch stochastic demand and distributed generation is using point predictions of its realization. However, one should also account that the battery might not have enough up/downward regulation capacity to compensate for deviations, e.g. because the battery is completely discharged at the end of the day of operations. In this case, it is necessary to recharge the battery to make sure that a suitable level of flexibility is restored to cope with intra-day uncertainty. Following this reasoning and inspired from [3], we define the dispatch plan as the sum of two terms: the point predictions of the power flow at the grid connection point, denoted by $\hat{\mathbf{L}} = \hat{L}_1, \ldots, \hat{L}_N$ and an offset power profile, $\mathbf{F} = F_1, \ldots, F_N$:

$$\hat{P}_k = \hat{L}_k + F_k \text{ for } k = 1, \ldots, N. \tag{3.1}$$

By embedding the offset profile into the dispatch plan, we implicitly account for the energy to manage the battery's state-of-charge, thus without the need of developing a parallel mechanism to charge or discharge the battery. The way the offset profile is computed is explained in the following. We obtain, with a forecasting tool from the literature [3], the daily forecasted profile of the feeder prosumption as well as the deviations from the forecasted profile in the highest and lowest demand scenarios, denoted by $\mathbf{L}^{\uparrow} = L_1^{\uparrow}, \ldots, L_N^{\uparrow}$ and $\mathbf{L}^{\downarrow} = L_1^{\downarrow}, \ldots, L_N^{\downarrow}$. The maximum positive and negative BESS power requirements for the dispatch service are therefore defined as the sum over k of the offset power F_k and of $L_k^{\uparrow}$ and $L_k^{\downarrow}$, respectively. With respect to the general definitions of x and θ given Section 2, the terms $L_k^{\uparrow}$ and $L_k^{\downarrow}$ are input quantities (i.e. $\{\mathbf{L}^{\uparrow}, \mathbf{L}^{\downarrow}\}$ are in θ) whereas the offset power $\mathbf{F}$ is a decision variable, determined by the optimization problem defined hereafter (i.e. $\mathbf{F}$ is in x). The power budget is therefore defined as:

$$\mathcal{P}_D = \{\left[P_{D,k}^{\downarrow}(x,\theta), P_{D,k}^{\uparrow}(x,\theta)\right], k = 1, \ldots, N\} = \{\left[F_k + L_k^{\downarrow}, F_k + L_k^{\uparrow}\right], k = 1, \ldots, N\} \tag{3.2}$$

The associated energy budget is:

$$\mathcal{E}_D = \{\left[E_{D,k}^{\downarrow}(x,\theta), E_{D,k}^{\uparrow}(x,\theta)\right], k = 1, \ldots, N\} s = \left[\frac{T}{N}\sum_{i=1}^{k}(F_i + L_i^{\downarrow}), \frac{T}{N}\sum_{i=1}^{k}(F_i + L_i^{\uparrow})\right] \tag{3.3}$$

with $k = 1, \ldots, N$.

The primary frequency regulation service requires the battery to provide a power proportional to the deviation of the frequency from its nominal value $\Delta f_k = f_k - f_n$ [29], with a proportionality coefficient hereafter denoted by α:

$$P_{FR,k} = \alpha \Delta f_k = \alpha \left(f_k - f_n\right). \tag{3.4}$$

The unit of measurement of α is kW/Hz. The instantaneous requested power cannot be forecasted since frequency deviations are difficult to predict. Therefore, the power budget required by this application will correspond to a constant profile, equal to the maximum power that frequency regulation may require. Since grid codes typically require complete activation of primary reserves for frequency deviations of more than $\Delta f_{max} = 200$ mHz [29], the power budget can be defined as:

$$\mathcal{P}_{FR} = \left\{\left[P_{FR,k}^{\downarrow}(x,\theta), P_{FR,k}^{\uparrow}(x,\theta)\right], k = 1, \ldots, N\right\} = \left[-0.2\alpha \cdot \mathbf{1}, 0.2\alpha \cdot \mathbf{1}\right], \tag{3.5}$$

where $\mathbf{1}$ is the all-one vector of length N. The energy budget necessary to ensure feasible operation for this service within a given time interval can be inferred statistically. In particular, we examined grid frequency data of the European grid from the last 2 years. Data have been collected by a PMU-based metering system installed on the EPFL campus [30]. Since frequency regulation requires the injection of a power $P_k = \alpha \Delta f_k$, the energy required by the grid during a given time window T is:

$$E_{FR,k} = \frac{T}{N} \sum_{i=0}^{k} P_{FR,i} = \frac{T}{N} \sum_{i=0}^{k} (\alpha \Delta f_i) = \alpha \left(\frac{T}{N} \sum_{i=0}^{k} \Delta f_i \right) = \alpha W_{f,k} \tag{3.6}$$

for $k = 1, \ldots, N$ and where $W_{f,k}$ denotes the integral of frequency deviations over a period of time and it is to be interpreted as the *energy content* of the signal given by the frequency deviation from its nominal value. The upper and lower bounds for $W_{f,k}$ for $k = 1, \ldots, N$ can be inferred from a statistical analysis of historical frequency deviation time-series (reported in Appendix B). These are defined hereafter as $\mathbf{W}_f^{\uparrow} = W_{f,1}^{\uparrow}, \ldots, W_{f,N}^{\uparrow}$ and $\mathbf{W}_f^{\downarrow} = W_{f,1}^{\downarrow}, \ldots, W_{f,N}^{\downarrow}$. With regard to the general definitions of x and θ given in Section 2, the terms $W_k^{\uparrow}$, $W_k^{\downarrow}$ (as well as Δf_{max} in (3.5)) are input quantities (i.e. $\{\mathbf{W}^{\uparrow}, \mathbf{W}^{\downarrow}, \Delta f_{max}\}$ are in θ) whereas α is a decision variable, determined by the optimization problem defined hereafter (i.e. α is in x). The energy budget for frequency regulation is then defined as:

$$\mathcal{E}_{FR} = \left\{ \left[E_{FR,k}^{\downarrow}(x,\theta), E_{FR,k}^{\uparrow}(x,\theta) \right], k = 1, \ldots, N \right\} = \left\{ \left[\alpha W_{f,k}^{\downarrow}, \alpha W_{f,k}^{\uparrow} \right], k = 1, \ldots, N \right\} \tag{3.7}$$

3.1.2. Formulation of the optimization problem

With reference to the formulation of the optimization problem in (2.5)-(2.7), let the decision vector x and the vector of controllers parameters θ be defined as $x = [\alpha, \mathbf{F}]$ and $\theta = [\Delta f_{max}, \mathbf{W}_f^{\downarrow}, \mathbf{W}_f^{\uparrow}, \mathbf{L}^{\downarrow}, \mathbf{L}^{\uparrow}]$. The energy budget consists of the demand required by the dispatch action and PFR. Therefore, the vector of the objective function in (2.5) is:

$$w \left(\sum_j \mathcal{E}_j \right) = w \left(\mathcal{E}_D + \mathcal{E}_{FR} \right). \tag{3.8}$$

The k-th element of the vector above can be expressed as the difference between the upper bound of the energy demand and the lower bound, thus:

$$= \left(\frac{T}{N} \sum_{i=0}^{k} (F_i + L_i^{\uparrow}) + \alpha W_{f,k}^{\uparrow} \right) - \left(\frac{T}{N} \sum_{i=0}^{k} (F_i + L_i^{\downarrow}) + \alpha W_{f,k}^{\downarrow} \right) = \tag{3.9}$$

$$= \frac{T}{N} \sum_{i=0}^{k} \left(L_i^{\uparrow} - L_i^{\downarrow} \right) + \alpha \left(W_{f,k}^{\uparrow} - W_{f,k}^{\downarrow} \right) \tag{3.10}$$

Since α is the only control variable in the expression above, the objective of maximizing the norm of $w \left(\sum_j \mathcal{E}_j \right)$ in (2.5) reduces to maximizing α, subject to (2.6) and (2.7). Finally, the problem (2.5)-(2.7) cast to the case of PFR with dispatch is:

$$[\alpha^o, \mathbf{F}^o] = \underset{\alpha \in \mathbb{R}^+, \mathbf{F} \in \mathbb{R}^N}{\arg\max} \ (\alpha) \tag{3.11}$$

subject to:

$$E_{init} + \mathcal{E}_D(x,\theta) + \mathcal{E}_{FR}(x,\theta) \in [E_{min}, E_{max}] \tag{3.12}$$
$$\mathcal{P}_D(x,\theta) + \mathcal{P}_{FR}(x,\theta) \in [-P_{max}, P_{max}] \tag{3.13}$$

By expressing explicitly the dependency of the power and energy budgets on the parameters and control variables, the problem (3.11)-(3.13) becomes:

$$[\alpha^o, \mathbf{F}^o] = \underset{\alpha\in\mathbb{R}^+, \mathbf{F}\in\mathbb{R}^N}{\arg\max} \ (\alpha) \tag{3.14}$$

subject to:

$$E_{init} + \frac{T}{N}\sum_{i=1}^{k}\left(F_i + L_i^{\uparrow}\right) + \alpha W_{f,k}^{\uparrow} \leq E_{max} \tag{3.15}$$
$$E_{init} + \frac{T}{N}\sum_{i=1}^{k}\left(F_i + L_i^{\downarrow}\right) + \alpha W_{f,k}^{\downarrow} \geq E_{min} \tag{3.16}$$
$$F_k + L_k^{\uparrow} + 0.2\alpha \leq P_{max} \tag{3.17}$$
$$F_k + L_k^{\downarrow} + 0.2\alpha \geq -P_{max} \tag{3.18}$$

for $k = 1, \ldots, N$.

3.1.3. Determination of E_{min} to include the BESS efficiency

The notion of battery round-trip efficiency is incorporated in the decision problem (3.14)-(3.18) with an empirical two-stage approach by enforcing conservative limits for the battery stored energy. This process is explained in the following. First, the problem (3.14)-(3.18) is solved implementing the nominal battery state-of-energy limits (i.e. $E_{max} = E_{nom}$ and $E_{min} = 0$). Second, the following finite impulse response model [3, 31]:

$$E_k = E_0 + \frac{T}{N}\sum_{i=1}^{k}\eta_i B_i, \qquad \eta_i = \begin{cases} \beta & B_i \geq 0 \\ 1/\beta & B_i < 0 \end{cases}, \tag{3.19}$$

where B_i is the total power injected or absorbed by the BESS at time i and η_i the BESS efficiency, is used to model the stored energy E_k of a non ideal BESS for the set of simulation scenarios presented in Section 4.1. The energy stored at the end of each day in a BESS modeled as ideal ($\eta = 1$) and non ideal ($\eta = 0.96$[1]) are compared and the largest difference over the all set of simulations is used to impose a conservative bound to the minimum stored energy constraint (3.16). For example, in the case proposed in Section 4.1, the largest difference is 4% of E_{nom}, therefore we adopt $E_{min} = 0.05E_{nom}$. It is worth noting that this approach allows to define the energy budgets independently for each service and sum them as in (3.10). In other words, it achieves a separation of concerns between services, which can be designed independently from each other and stacked together at the end of the process. Also, it is worth noting that the round-trip efficiency of modern Li-ion based BESS is generally above 90% [32–34]. An accurate investigation of the modelling errors, considering also less efficient storage technologies (like fuel cells), is postponed to future works.

[1] the value of $\eta = 0.96$ has been determined experimentally for the 560 kWh/720 kVA BESS used in this work.

3.2. Real-time control

The proposed algorithm consists in solving a scheduling problem for the next calendar day of operation, determining the values of the coefficient α^o and of the offset profile $\mathbf{F}^o$ and in a real-time control problem. The latter is not the main contribution of the present work, however it is summarized hereafter and illustrated in Figure 3.2 for the sake of clarity. The real-time control determines the

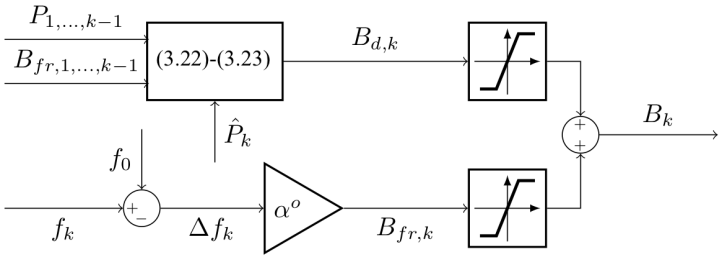

Figure 3.2: Scheme of the real-time control for the BESS.

battery active power setpoint B_k with 1-second resolution. In the following, the index k denotes the 1-second resolution time interval. B_k is the algebraic sum of the setpoints $B_{d,k}$ and $B_{fr,k}$ determined respectively for the dispatch and the PFR by two independent control loops:

$$B_k = B_{d,k} + B_{fr,k}. \tag{3.20}$$

The power setpoint $B_{d,k}$ is to compensate the tracking error ϵ_k, which is the difference between the objectve feeder power $\hat{P}_k$ (from the dispatch plan, with 5 minutes resolution) and the mean deviation from this value within the 5 minutes interval. This deviation is the sum of two terms. The first is the mean of the feeder power measurements P_i in the instants from the beginning of the current 5-minutes period and present, filtered out of the power requests due to the PFR, $B_{fr,i}$. The second is a short-term forecast of the load $\hat{L}_i$ over the remaining five minutes interval:

$$\epsilon_k = \hat{P}_k - \frac{1}{300}\left(\sum_{i=0}^{k-1}(P_i - B_{fr,i}) + \sum_{i=k}^{5\text{ min}} \hat{L}_i\right). \tag{3.21}$$

The expression above is an energy objective over a 5 minutes horizon and the power setpoint to respect it is therefore defined as:

$$B_{d,k} = \frac{1}{300-k} \cdot \epsilon_k. \tag{3.22}$$

The power setpoint for the frequency regulation $B_{fr,k}$ is calulated as:

$$B_{fr,k} = \alpha^o \cdot (f_k - f_n). \tag{3.23}$$

In order to comply with the constraints imposed by the day-ahead policy, both setpoints are constrained within saturation tresholds, which are, notably, equal to $\pm 0.2\alpha^o$ for $B_{fr,k}$ and $\pm(P_{max} - 0.2\alpha^o)$ for $B_{d,k}$. The latter threshold is set such that the dispatch can require, istantaneously, all the power not reserved by the frequency regulation. It remains, nevertheless, that the dispatch power averaged over a 5 minutes period is expected to remain between $\mathbf{L}^{\uparrow} + \mathbf{F}^o$ or $\mathbf{L}^{\downarrow} + \mathbf{F}^o$.

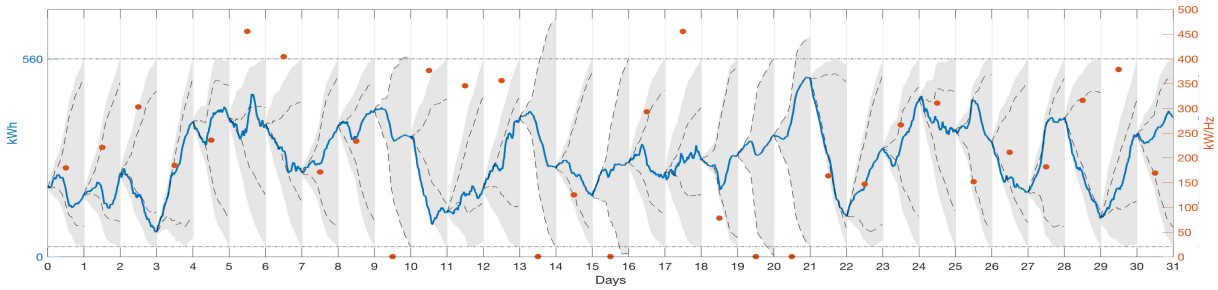

Figure 3.3: Simulation results of 31 consecutive days of operation. Blue line: BESS stored energy; Grey area: total daily energy budget $\mathcal{E}_D + \mathcal{E}_{FR}$; Black dashed lines: bounds of the daily energy budget reserved to the dispatching service $\mathcal{E}_D$; red dots: daily values of α^o (referred to the right-hand y-axis).

4.Results

The proposed planning and control strategy has been validated by simulations and experiments in a real-life grid.

The goal of this validation effort is double. The simulations demonstrate the effectiveness of the proposed control architecture in the determination of the coefficient α^o and of the offset profile $\mathbf{F^o}$. The values found for such quantities allow to maximise the battery exploitation, while respecting the battery operational limits and therefore allowing for the continuous operation for a month. The experimental results validate the assumptions made in the control design and in the simulations and demonstrate the practical relevance and deployability of the proposed control architecture.

Both simulations and experiments are based on a setup with a 560 kWh/720 kVA Lithium-ion BESS installed at the EPFL campus in Lausanne, Switzerland, and connected to a 20 kV medium voltage feeder. The feeder interfaces 5 office buildings (300 kW global peak demand) and rooftop PV installations (90 kWp). Both historical data used in the simulations and real-time measurements of the power flows and grid frequency are obtained via a PMU-based metering system [30].

4.1. Simulations

Thirty-one consecutive days of operation are simulated. These 31 days are characterised by different initial SOE values[1], ranging from 12% to 90%, and determined by the operation of the previous days (the first day of the simulation the initial SOE has been set to 35%).

Figure 3.3 reports the profile of the energy stored the battery along the 31 days and the daily energy budget for the dispatching service $\mathcal{E}_D$ and the total daily energy budget ($\mathcal{E}_D + \mathcal{E}_{FR}$), calculated as a function the stochastic forecasting model of the demand and frequency (i.e. on the basis of $[\mathbf{L}^{\uparrow}, \mathbf{L}^{\downarrow}, \mathbf{W}_f^{\uparrow}, \mathbf{W}_f^{\downarrow}]$). Figure 3.3 shows as well the values assumed daily by α^o. It can be observed that the total daily energy budgets (grey areas) hit the BESS operational limits (SOE=5% and SOE=100%) in all days except for day 10, 14, 16, 20 and 21. This denotes that the day-ahead planning problem is able to schedule efficiently the offset profile $\mathbf{F}^o$ and the value α^o to exploit the full battery energy capacity accounting for the stochastic behaviour of frequency and demand. On the other hand, in the five days mentioned above, the grey area exceeds the SOE limits. This is because the uncertainity related to the demand (reflected by the sequences $\mathbf{L}^{\uparrow}$ and $\mathbf{L}^{\downarrow}$) prevents the feasibility of problem

[1]The SOE is here defined as the amount of stored energy normalized over the BESS nominal energy capacity E_{nom}.

(3.11)-(3.13). In such days, the solution of (3.11)-(3.13) provides an α^o equal to zero, i.e. no frequency regulation is performed. In all cases, the activated constraint in the solution of (3.11)-(3.13) has been the one on the energy budget sum.

Quantitative results from the simulations are collected in Table 4.1: SOE_0 is the daily initial SOE in percentage, α^o the daily coefficient for PFR in kW/Hz, F_{avg} the mean value of the offset profile and ΔSOE the overall SOE variation during the day due to the simultaneous deployment of the two services. Table 4.1 shows the average, maximum and minimum values of such quantities over the 31 days simulation period. The average daily value of α^o is of 216.6 kW/Hz. This corresponds to the provision of up to 43 kW for PFR (considering Δf_{max} = 200 mHz). In comparison to the work by the same Authors in [3], where the control of the BESS aims exclusively at dispatching the operation of a MV feeder, we are able to provide power both for the dispatch and for PFR, while still ensuring the respect of the BESS operational constraints. This is done by taking advantage of the BESS capacity that remains unexploited by the dispatching operation, due to the daily variation of the uncertainty set of the prosumption defined by $\left[L_k^{\downarrow}, L_k^{\uparrow}\right]$ for $k = 1, \ldots, N$. The black dashed lines in Figure 3.3 delimit the energy budget reserved to the dispatching service $\mathcal{E}_D$. The width of this budget in days characterized by low uncertainty in the feeder prosumption forecast (e.g. days 5 or 17) is rather narrow and the unexploited battery capacity is therefore allocated to provide PFR (a high value of α^o is found). In days in which such uncertainty is high (e.g. days 18 to 20) almost all (or more than all) the battery capacity is needed to perform the dispatch, resulting in a very wide $\mathcal{E}_D$ and in a very low value of α^o.

Table 4.1: Simulation results over 31 days of operation.

	SOE_0 [%]	α^o [kW/Hz]	F_{avg} [kW]	$SOE_{min}\|_T$ [%]	$SOE_{max}\|_T$ [%]
Mean	50.8	216.6	0.5	37.4	64.9
Max	90.3	455.7	10.0	61.6	90.7
Min	12.5	0.0	-9.3	12.4	36.0

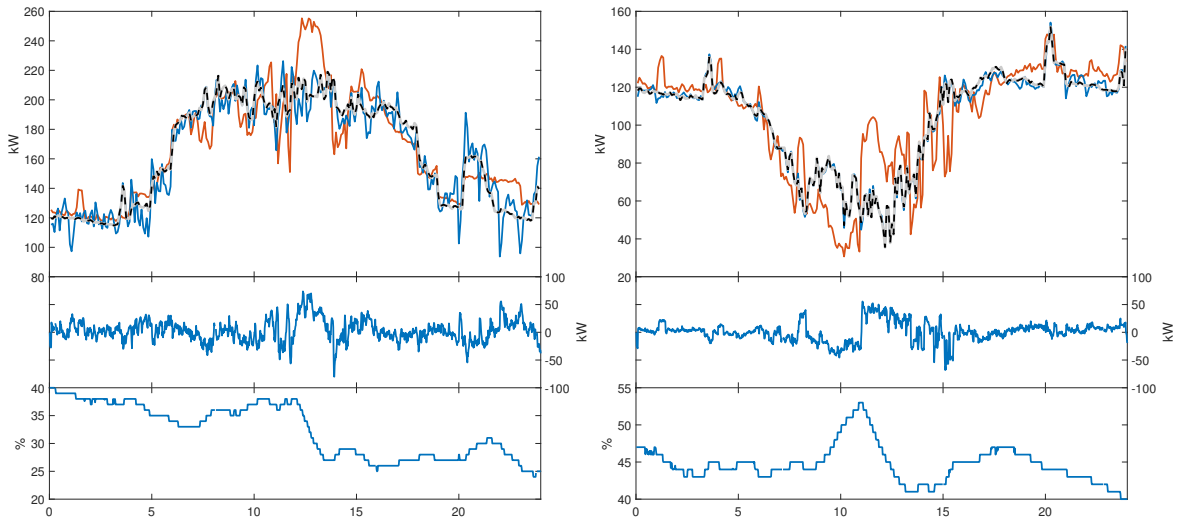

Figure 4.1: Experimental results, **left:** day 1, **right:** day 2. **Upper plots -** feeder power profiles. Thick grey line: dispatch plan, red line: feeder prosumption, dashed black line: feeder real power (excluded the PFR power injection), blue line: feeder real power (with the PFR). **Middle plots -** BESS power injection. **Lower plots -** BESS SOE evolution.

4.2. Experimental validation

The described algorithm has been implemented in the controller of the 560 kWh/720 kVA Lithium-ion BESS. The results of 2 days of experiments are reported in this section.

Figure 4.1 shows the power and SOE profiles for two days of operation, an intra-week day and a weekend day (hereafter referred to as Day 1 and Day 2). Numerical results are summarized in Table 4.2 and Table 4.3. In Day 1, the day-ahead optimization procedure has determined a value of α^o of 584 kW/Hz and an offset power of 0.84 kW on average. In Day 2, the α^o has been found equal to 127 kW/Hz and the average offset power equal to -0.56 kW. These values of α^o allow to exploit a portion of the battery capacity that would remain unexploited when providing power only to dispatch the operation of the MV feeder, as in [3]. In this case, the maximum amplitude of the energy budget that needs to be reserved for the dispatch, calculated as in (3.3) on the basis of the upper and lower worst case scenarios of the feeder prosumption ($L_k^{\downarrow}$ and $L_k^{\uparrow}$, with $k = 1, \ldots, N$), is of about the 54% of the BESS nominal capacity for Day 1 and of about the 10% for Day 2. The remaining capacity is fully exploited by the PFR application, thanks to the computation of a proper value of α^o, by means of (3.11)-(3.13).

Table 4.3 collects the relevant metrics to evaluate the performance of the dispatch application when performed in conjunction with frequency regulation, i.e. the mean, RMS and maximum absolute values of the tracking error in these two days. The RMS value of the tracking error is about 0.5 kW over a feeder prosumption of about 130 kW on average.

Table 4.2: Experimental results for two days of operation.

	SOE_0 [%]	α^o [kW/Hz]	F_{avg} [kW]	$SOE_{min}\|_T$ [%]	$SOE_{max}\|_T$ [%]
Day 1	40	584	0.84	24	40
Day 2	47	127	-0.56	40	53

Table 4.3: Metrics on dispatch performance (in kW).

	ϵ_{mean}	ϵ_{rms}	ϵ_{max}
Day 1	-0.03	0.52	4.45
Day 2	0.02	0.5	6.83

We note that, in both these two days, the energy demand for the two applications has been of opposite sign. For istance, in Day 1 the daily energy requested for the dispatch operation is of about 89 kWh, whereas the average power requested for the frequency regulation is of -24 kWh. The simultaneous deployment of these two services in this case generates a SOE drift that is lower than the one the dispatch alone would generate. It is worth noting that, when simultaneously providing multiple services, the saturation (or depletion) of the battery energy capacity would occur only if the power requests of all services corresponded to the upper (or lower) bounds of their budgets. If the uncertain processes related to the services are uncorrelated, as in the case of the dispatch and frequency regulation, the occurrence of this condition is reduced. Providing multiple services simultaneously, in this regard, may ensure more reliable operation, in the sense that failure due to complete depletion or saturation of the battery capacity would be less likely to occur. The downside of this is of course that an eventual failure would be more deleterious since multiple services would stop at once. This could be addressed by implementing strategies to prioritize the services in contingency situations, e.g. by selecting, before hitting the operational limits, which service is to drop and which to maintain.

5.Integration of grid forming strategies in the proposed formulation

By leveraging the notion of composability of the power and energy budgets in (2.7) and (2.6), any service for which it is possible to determine those can be added in the scheduling algorithm. In the case of dispatch and primary frequency regulation, the power and energy budgets were computed by a suitable forecasting engine and on the basis of statistics performed on historical data, respectively. In the case of synchronization and grid forming algorithms, the budgets can be estimated similarly to primary frequency regulation if historical operational data are available, or with a conservative approach by devoting pre-determined fixed amounts of energy capacity and power converter limits. The development of suitable forecasting tools to capture the power and energy demand of grid synchronization and grid forming algorithms will be addressed in a future research, however not in the context of this European project.

6.Conclusion

We have proposed an algorithm to schedule and control the operation of a battery energy storage system to provide multiple services simultaneously. Its objective is maximising the battery capacity exploitation in the presence of variable and stochastic energy and power requirements.

The proposed control consists in two phases. First, in the operation-scheduling phase the portion of battery power and energy capability to be allocated for each service is determined. This is accomplished by an optimization that takes into account the uncertainty in the forecasted power and energy requirements of each service. Second, in the real-time phase the different services are deployed by injecting in the grid a real power corresponding to the sum of the power setpoints of the individual services.

The algorithm is first formulated in generic terms and then casted to the case of providing BESS power to simultaneously dispatch the active power flow of a distribution network and provide primary frequency regulation to the grid. For these two services the power and energy budgets are modelled in the planning problem by predictions delivered by forecasting tools. The solution of the operation-scheduling optimization problem provide, on a daily basis, the maximum value of the PFR regulating power that can be deployed while respecting the battery operational constraints. It provides moreover the offset profile, i.e. the power needed, on a daily basis to restore the stored energy to a level that ensures continuous operation.

The proposed control scheme is validated by simulations and experimentally. Simulations are obtained by applying the proposed scheme to a set of load and frequency data measured on-site and corresponding to one month of operation. Simulation results show that the proposed scheme does ensure continuous operation and does determine the maximum possible frequency regulating power that can be provided in conjunction to the dispatch application. Experiments are performed on a real-life grid by using a grid-connected 560 kWh/720 kVA lithium titanate BESS, connected to a medium voltage grid interfacing a set of office buildings and PV generating units. Results from 2 days of operations are shown and demonstrate the deployability of the proposed control scheme. In these two days of operation, a regulating power up to 117 and 25 kW respectively can be provided on top of the dispatch operation. The latter is performed with a RMS tracking error of about 0.5 kW.

A.Economic optimization and feasibility problems

The objective of the cost function (2.5) is maximising the battery energy capacity exploited during a period of operation T. The same framework can be exploited to optimise the BESS operation consid-

ering different objectives. For instance, one could seek the value of x that maximises the economical benefit of providing multiple concurrent services via an optimization function such as:

$$x^o = \arg\max_x \sum r_j \tag{A.1}$$

subject to (2.6), (2.7) and:

$$r_j = f_j(\mathcal{E}_j, \mathcal{P}_j) \tag{A.2}$$

where r_j is the revenue that the application j can generate in period T, and is a function of the energy and power budgets reserved for that service. Similarly, if the objective is simply to find a value for x that ensures feasible operation, one could write:

$$x^o = \arg\max_x \quad 1 \tag{A.3}$$

subject to (2.6) (2.7).

B.Computation of BESS energy needs for PFR

The terms $\mathbf{W}_f^{\downarrow}$ and $\mathbf{W}_f^{\uparrow}$ are computed on the basis of a statistical analysis of past data from the last two years of frequency deviations and assuming that the BESS under control does not influence the future frequency deviation. First, the daily profiles composed by $\mathbf{W}_f = W_{f,1}, \ldots, W_{f,N}$ have been calculated from hystorical data, by integrating the frequency deviations measured in a set of 24 h periods. The mean $\mu_{W,k}$ and variance $\sigma^2_{W,k}$ of such values have then been computed for all $k = 1, \ldots, N$. It can be observed that the set of $W_{f,k}$ values is close to normally distributed for any instant k. A Chi-square goodness-of-fit test on the dataset does in fact not reject the null hypothesis at the 5% significance level. In Fig. B.1, it is shown that the normal probability plot of the values assumed $W_{f,k}$ for $k = N$ (i.e. at the end of the 24 hours). We then define $W^{\uparrow}_{f,k}$ and $W^{\downarrow}_{f,k}$ for all k as a function of the mean value $\mu_{W,k}$ and the standard deviation $\sigma_{W,k}$ as

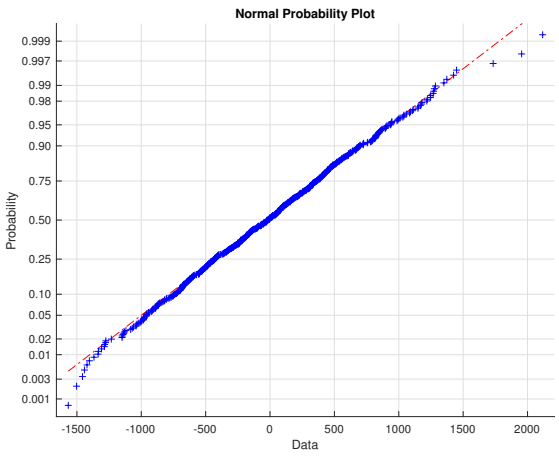

Figure B.1: Normal probability plot of $W_{f,N}$.

$$\begin{aligned} W^{\uparrow}_{f,k} &= \mu_{W,k} + 1.96\sigma_{W,k} \\ W^{\downarrow}_{f,k} &= \mu_{W,k} - 1.96\sigma_{W,k}, \text{ for } k = 1, \ldots, N \end{aligned} \tag{B.1}$$

to have a 95% confidence level that the realization of $W_{f,k}$ will lie between $W_{f,k}^{\uparrow}$ and $W_{f,k}^{\downarrow}$. Similarly, we can define $W_{f,k}^{\uparrow}$ and $W_{f,k}^{\downarrow}$ for any other confidence level.

Bibliography

[1] A. Oudalov, R. Cherkaoui, and A. Beguin, "Sizing and optimal operation of battery energy storage system for peak shaving application," in *Power Tech, 2007 IEEE Lausanne*. IEEE, 2007, pp. 621–625.

[2] B. Belvedere, M. Bianchi, A. Borghetti, C. A. Nucci, M. Paolone, and A. Peretto, "A microcontroller-based power management system for standalone microgrids with hybrid power supply," *IEEE Transactions on Sustainable Energy*, vol. 3, no. 3, pp. 422–431, 2012.

[3] F. Sossan, E. Namor, R. Cherkaoui, and M. Paolone, "Achieving the dispatchability of distribution feeders through prosumers data driven forecasting and model predictive control of electrochemical storage," *IEEE Transactions on Sustainable Energy*, vol. 7, no. 4, pp. 1762–1777, 2016.

[4] X. Ke, N. Lu, and C. Jin, "Control and size energy storage systems for managing energy imbalance of variable generation resources," *IEEE Transactions on Sustainable Energy*, vol. 6, no. 1, pp. 70–78, 2015.

[5] K. Christakou, D.-C. Tomozei, M. Bahramipanah, J.-Y. Le Boudec, and M. Paolone, "Primary voltage control in active distribution networks via broadcast signals: The case of distributed storage," *IEEE Transactions on Smart Grid*, vol. 5, no. 5, pp. 2314–2325, 2014.

[6] A. Oudalov, D. Chartouni, and C. Ohler, "Optimizing a battery energy storage system for primary frequency control," *IEEE Transactions on Power Systems*, vol. 22, no. 3, pp. 1259–1266, 2007.

[7] E. Hittinger, J. Whitacre, and J. Apt, "What properties of grid energy storage are most valuable?" *Journal of Power Sources*, vol. 206, pp. 436–449, 2012.

[8] G. Denis, T. Prevost, M. Debry, F. Xavier, X. Guillaud, and A. Menze, "The migrate project: the challenges of operating a transmission grid with only inverter-based generation. a grid-forming control improvement with transient current-limiting control," *IET Renewable Power Generation*, vol. 12, no. 5, pp. 523–529, 2018.

[9] D. Wu, C. Jin, P. Balducci, and M. Kintner-Meyer, "An energy storage assessment: Using optimal control strategies to capture multiple services," in *Power & Energy Society General Meeting, 2015 IEEE*. IEEE, 2015, pp. 1–5.

[10] J. Eyer and G. Corey, "Energy storage for the electricity grid: Benefits and market potential assessment guide," *Sandia National Laboratories*, vol. 20, no. 10, p. 5, 2010.

[11] B. Wasowicz, S. Koopmann, T. Dederichs, A. Schnettler, and U. Spaetling, "Evaluating regulatory and market frameworks for energy storage deployment in electricity grids with high renewable energy penetration," in *European Energy Market (EEM), 2012 9th International Conference on the*. IEEE, 2012, pp. 1–8.

[12] M. Kazemi and H. Zareipour, "Long-term scheduling of battery storage systems in energy and regulation markets considering battery's lifespan," *IEEE Transactions on Smart Grid*, 2017.

[13] M. Kazemi, H. Zareipour, N. Amjady, W. D. Rosehart, and M. Ehsan, "Operation scheduling of battery storage systems in joint energy and ancillary services markets," *IEEE Transactions on Sustainable Energy*, 2017.

[14] E. Drury, P. Denholm, and R. Sioshansi, "The value of compressed air energy storage in energy and reserve markets," *Energy*, vol. 36, no. 8, pp. 4959–4973, 2011.

[15] B. Cheng and W. Powell, "Co-optimizing battery storage for the frequency regulation and energy arbitrage using multi-scale dynamic programming," *IEEE Transactions on Smart Grid*, 2016.

[16] O. Mégel, J. L. Mathieu, and G. Andersson, "Scheduling distributed energy storage units to provide multiple services under forecast error," *International Journal of Electrical Power & Energy Systems*, vol. 72, pp. 48–57, 2015.

[17] E. Vrettos and G. Andersson, "Combined load frequency control and active distribution network management with thermostatically controlled loads," in *Smart Grid Communications (SmartGridComm), 2013 IEEE International Conference on*. IEEE, 2013, pp. 247–252.

[18] Y. Shi, B. Xu, D. Wang, and B. Zhang, "Using battery storage for peak shaving and frequency regulation: Joint optimization for superlinear gains," *arXiv preprint arXiv:1702.08065*, 2017.

[19] X. Xi, R. Sioshansi, and V. Marano, "A stochastic dynamic programming model for co-optimization of distributed energy storage," *Energy Systems*, vol. 5, no. 3, pp. 475–505, 2014.

[20] R. Moreno, R. Moreira, and G. Strbac, "A milp model for optimising multi-service portfolios of distributed energy storage," *Applied Energy*, vol. 137, pp. 554–566, 2015.

[21] A. Perez, R. Moreno, R. Moreira, M. Orchard, and G. Strbac, "Effect of battery degradation on multi-service portfolios of energy storage," *IEEE Transactions on Sustainable Energy*, vol. 7, no. 4, pp. 1718–1729, 2016.

[22] M. Nick, R. Cherkaoui, and M. Paolone, "Optimal allocation of dispersed energy storage systems in active distribution networks for energy balance and grid support," *IEEE Transactions on Power Systems*, vol. 29, no. 5, pp. 2300–2310, 2014.

[23] H. Zhao, Q. Wu, S. Hu, H. Xu, and C. N. Rasmussen, "Review of energy storage system for wind power integration support," *Applied Energy*, vol. 137, pp. 545–553, 2015.

[24] H. Akhavan-Hejazi and H. Mohsenian-Rad, "Optimal operation of independent storage systems in energy and reserve markets with high wind penetration," *IEEE Transactions on Smart Grid*, vol. 5, no. 2, pp. 1088–1097, 2014.

[25] F. Brahman, M. Honarmand, and S. Jadid, "Optimal electrical and thermal energy management of a residential energy hub, integrating demand response and energy storage system," *Energy and Buildings*, vol. 90, pp. 65–75, 2015.

[26] S. Shafiee, M. Fotuhi-Firuzabad, and M. Rastegar, "Impacts of controlled and uncontrolled phev charging on distribution systems," 2012.

[27] H. Mohsenian-Rad, "Coordinated price-maker operation of large energy storage units in nodal energy markets," *IEEE Transactions on Power Systems*, vol. 31, no. 1, pp. 786–797, 2016.

[28] ——, "Optimal bidding, scheduling, and deployment of battery systems in california day-ahead energy market," *IEEE Transactions on Power Systems*, vol. 31, no. 1, pp. 442–453, 2016.

[29] B. Xu, A. Oudalov, J. Poland, A. Ulbig, and G. Andersson, "Bess control strategies for participating in grid frequency regulation," *IFAC Proceedings Volumes*, vol. 47, no. 3, pp. 4024–4029, 2014.

[30] M. Pignati, M. Popovic, S. Barreto, R. Cherkaoui, G. D. Flores, J.-Y. Le Boudec, M. Mohiuddin, M. Paolone, P. Romano, S. Sarri *et al.*, "Real-time state estimation of the epfl-campus medium-voltage grid by using pmus," in *Innovative Smart Grid Technologies Conference (ISGT), 2015 IEEE Power & Energy Society*. IEEE, 2015, pp. 1–5.

[31] P. Fortenbacher, A. Ulbig, and G. Andersson, "Optimal placement and sizing of distributed battery storage in low voltage grids using receding horizon control strategies," *IEEE Transactions on Power Systems*, 2017.

[32] H. Qian, J. Zhang, J.-S. Lai, and W. Yu, "A high-efficiency grid-tie battery energy storage system," *IEEE transactions on power electronics*, vol. 26, no. 3, pp. 886–896, 2011.

[33] A. Castillo and D. F. Gayme, "Grid-scale energy storage applications in renewable energy integration: A survey," *Energy Conversion and Management*, vol. 87, pp. 885–894, 2014.

[34] P. Fortenbacher, J. L. Mathieu, and G. Andersson, “Modeling, identification, and optimal control of batteries for power system applications,” in *Power Systems Computation Conference (PSCC), 2014*. IEEE, 2014, pp. 1–7.